Available online at www.sciencedirect.com
SCIENCE DIRECT®
ELSEVIER
Journal of Magnetism and Magnetic Materials 258–259 (2003) 382–387
Journal of magnetism and magnetic materials
www.elsevier.com/locate/jmmm

Ordering in magnetic multilayers by off-specular neutron scattering

V. Lauter-Pasyuk[a,b,*], H.J. Lauter[c], B. Toperverg[d,e], L. Romashev[f], M. Milyaev[f], A. Petrenko[b], V. Aksenov[b], V. Ustinov[f]

[a] *Physik Department, TU.München, D-85747 Garching, Germany*
[b] *Joint Institute for Nuclear Research, 141980 Dubna, Moscow Region, Russia*
[c] *Institute Laue Langevin, B.P. 156,F-38042 Grenoble Cedex 9, France*
[d] *Forschungszentrum Jülich, IFF, D-52425 Jülich, Germany*
[e] *Petersburg Nuclear Physics Institute, Gatchina, 188350 St. Petersburg, Russia*
[f] *Institute of Metal Physics, Ural Div. Russian Academy Sciences, GSP-170 18 S. Kovalevskaya Str., 62019 Ekaterinburg, Russia*

Abstract

The combination of specular reflection and off-specular scattering with polarized neutrons gives a unique detailed information on the lateral and transverse spin-configuration of a magnetic multilayer stack. We present the first direct experimental observation of a phenomenon predicted theoretically for antiferromagnetically coupled multilayers: the twisted ground-state configuration in an external magnetic field. This twisted configuration arises due to the reduced symmetry of magnetic moments of the end layers having only one neighbor. This fact can be established *directly* via the *qualitative* analysis of the line shape of the superstructure peaks on the specular line and the related off-specular Bragg sheet. Additional *quantitative* evaluation of both specular reflection and off-specular scattering allows one to deduce the layer-by-layer spin configuration through the multilayer stack, as well as within the plane of the layer. The presence of spin-flip off-specular scattering means that the layer magnetization is laterally not homogeneous but is decomposed into a set of domains. The distribution of magnetic moments within each domain, the domains size and their distributions are obtained.

Keywords: Neutron reflection—polarized; Thin film—multilayers; Exchange coupling—non-collinear

1. Introduction

The phenomenon of the giant magnetoresistance in magnetic multilayers [1,2] exists for a wide variety of magnetic films with different spacer layers. A large change in resistance is connected to the change of the alignment of the layer magnetization and depends on their relative orientation. Several reviews have been written about the physical origin of the interlayer exchange coupling [3–5], describing several different models for the coupling. These models have some common features, like, for example, the period of the coupling. Other features, like the strength of the coupling, are different from model to model. However, as it was emphasized in Ref. [6], an accurate determination of the coupling requires an accurate and reliable determination of the magnetic moments orientation in each layer. The problem of the ground-state spin configuration of a finite multilayer composed of antiferromagnetically coupled ferromagnetic layers exposed to an in-plane external magnetic field was treated theoretically. The theory of the spin configurations as a function of the external fields, was realized for a two-fold anisotropy case [7] and the isotropic case [8].

The magnetic ordering in magnetic multilayers was experimentally studied by means of magnetometry, magneto-optics, etc. [3,9,10]. However, these methods

*Corresponding author. Fax: +33-4-76-20-71-20.
E-mail address: vlauter@ill.fr (V. Lauter-Pasyuk).

0304-8853/03/$ - see front matter
PII: S0304-8853(02)01118-6

can provide only integral characteristics of the multilayer and do not allow for the selective determination of magnetic properties of the buried layers. Also polarized neutron reflectometry (PNR) was used to determine the coupling angle from specular reflection (see review in Ref. [11]), when the magnetic structure was obtained through a model fit to the reflectivity line, neglecting the off-specular scattering. However, in this case one should be sure that the signal measured at specular conditions is the true coherent reflection and is not significantly contaminated by diffuse scattering. Meanwhile, rather strong diffuse scattering from exchange coupled multilayers is found being measured in off-specular directions [12,13]. Then, a complete evaluation of the data is required [12], but some valuable information, such as the mean angle between sublattice magnetization and external field can easily be obtained [14,15] analysing some features of off-specular scattering even without treatment of the whole data set.

In the present paper, we show that the polarized neutron specular reflection and off-specular scattering provides a unique detailed information on the spin-configuration through the multilayer stack. We present the direct experimental observation of a phenomenon existing in antiferromagnetically coupled multilayers: the twisted ground-state configuration in the external magnetic field. This twisted configuration appears due to the reduced symmetry of magnetic moments of the end layers having only one magnetic neighbor layer. We show that in finite superlattices the presence of two surfaces influences the configuration of magnetic moments through the entire multilayer. From the two-dimensional (2D) data analysis of specular reflection and off-specular scattering of polarized neutrons, the layer-by-layer spin configuration through the multilayer stack, as well as in-plane magnetic structure was obtained. It is shown that in-plane magnetization is not uniform but decomposed into a set of lateral domains, in which magnetic moments across the multilayer stack are arranged into a configuration confirming the theoretical calculations [7,8].

2. Experiment

A series of (0 0 1) $[^{57}Fe/Cr]_n$ superlattices with various thicknesses of Fe and Cr layers and number of bilayers were grown with molecular beam epitaxy on (1 1 0) Al_2O_3 substrates covered with a Cr buffer layer. The samples were characterized in situ with reflection high-energy electron diffraction (RHEED) and ex situ with X-ray diffraction. The in-plane magnetization measurements were performed at room temperature with a vibrating sample magnetometer (VSM) and show extremely strong in-plane anisotropy [16]. The magnetization curves were measured in different magnetic field orientations and show a four-fold in-plane anisotropy typical for (0 0 1) Fe/Cr systems.

The PNR experiments were carried out at the Institute Laue Langevin (Grenoble) on the ADAM and D17 spectrometers [17] operating both in monochromatic mode with the neutron wavelength λ of 4.41 Å and 11 Å, respectively, and polarization efficiency of 97%. The reflected and scattered intensities were recorded with 2D multidetectors. The external magnetic field was applied parallel to the sample surface. The scheme of the experiment is shown in Fig. 1.

Although we investigated a series of samples, we will concentrate in this article on two multilayers: [Cr(9 Å)/^{57}Fe(67 Å)]$_{12}$/Cr(68 Å)/Al_2O_3 (sample 1) and Cr(70 Å)/[^{57}Fe(26 Å)/Cr(14 Å)]$_{15}$/^{57}Fe(26 Å)/Cr(70 Å)/Al_2O_3 (sample 2). Both samples show antiferromagnetic coupling.

Fig. 2a depicts the scattered intensity from sample 1 in an external magnetic field of $H = 400$ G applied along the easy axis (0 0 1). The data are presented in a 2D map with scattered intensity in a gray log-scale shown at the right-hand side of the figure. The coordinate system is $(p_i + p_f)$ and $(p_i - p_f)$, with p_i and p_f the perpendiculars to the surface projections of incoming and scattered neutron wave-vectors, respectively. The neutron wave-vector is determined by the neutron wavelength λ and the scattering angle α, so that $p_{i,f} = 2\pi \sin \alpha_{i,f}/\lambda$ (see scattering geometry in Fig. 1). The specularly reflected intensity along the line $Q_z = (p_i + p_f)$ at $(p_i - p_f) = 0$

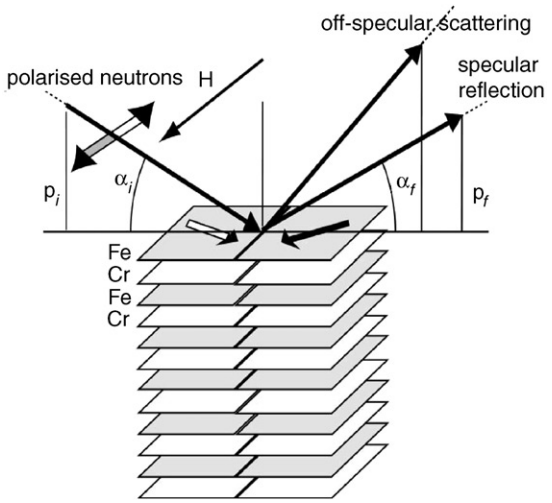

Fig. 1. Schematic presentation of an exchange coupled multilayer stack in an external in-plane magnetic field H and the scattering geometry of the neutron experiment. The polarized neutron beam with the incident angle α_i scatters from the sample in specular and off-specular directions with outgoing angles α_f. p_i and p_f are the perpendicular to the surface projections of incoming and scattered neutron wave-vectors, respectively.

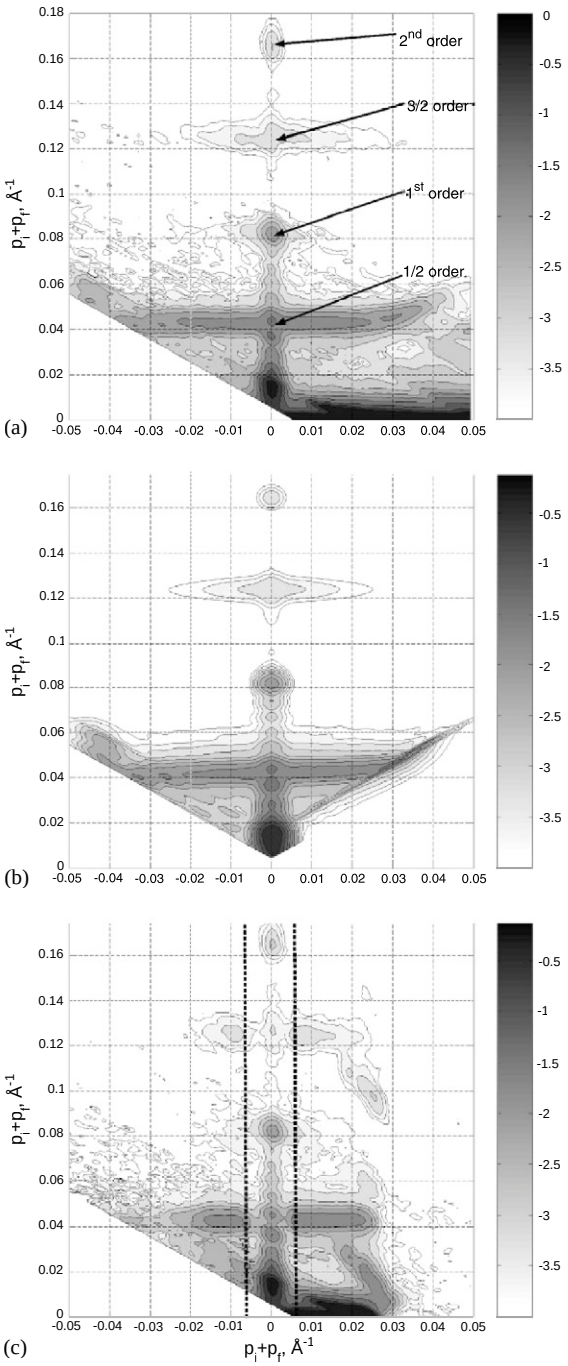

Fig. 2. (a) Experimental 2D map of the intensity scattered from sample 1 in an external magnetic field of $H = 400$ G as a function of $(p_i + p_f)$ and $(p_i - p_f)$, with p_i and p_f the perpendicular projections of incoming and scattered neutron wave-vectors, respectively. The logarithmic intensity gray-color scale is shown on the side. The incoming neutrons are in the "-" state (neutron spin is antiparallel to the direction of the external field). (b) 2D-model fit to the experimental data in Fig. 1a. (c) Experimental 2D intensity map with the analysed region between the dashed lines for the "–" state (non-spin-flip intensity).

shows the total thickness oscillations and the first-order Bragg peak at $(p_i + p_f) = 0.0826\,\text{Å}^{-1}$, where Q_z is the wave-vector transfer component normal to the surface. The positions of the first- and second-order Bragg peaks correspond to the bi-layer thickness of 76 Å. The $\frac{1}{2}$-order Bragg peak around $(p_i + p_f) = 0.0413\,\text{Å}^{-1}$ is due to the doubling of the unit cell perpendicular to the surface and has some very prominent features. The first remarkable phenomenon is that in the position of the superstructure Bragg peak along the specular line, the intensity is split into two peaks with a minimum in the middle. At the same time a strong off-specular scattering in the form of Bragg-sheet is concentrated exactly in the position of the superstructure Bragg peak and thus crosses the specular line at the minimum of the split superstructure Bragg peak. Additional measurements with polarization analysis of the scattered beam show that the intensity of the double superstructure Bragg peak has a non-spin-flip origin. In contrast, the intensity of the off-specular Bragg-sheet is spin-flipped. The data obtained with polarization analysis are shown in Fig 2c. The analyzed scattered beam region limited by the cross-section of the analyzer is marked with dashed lines. The presence of the off-specular scattering sheet in the $\frac{1}{2}$-order Bragg peak position manifests clearly the coexistence of non-collinear ordering with an in-plane domain structure [12,14]. This means that the sample is decomposed into vertical domains of an in-plane size smaller than the lateral coherence length of the neutrons and that there is within each domain a non-collinear alignment of magnetic moments in alternating Fe layers. As concerning the appearance of the superstructure Bragg peak in the non-spin-flip channel, this phenomenon occurs with a doubling of the structure through the multilayer stack.

3. Data analysis and discussion

Examples of configurations of magnetic moments in a multilayer stack are shown in Fig. 3 for antiferromagnetic (a), non-collinear (b) configurations in zero magnetic field and an in-pane external magnetic field (c). The interplay between the crystalline anisotropy and interlayer exchange coupling leads to the result that the layer magnetization vectors $\mathbf{M}^l$ in successive Fe layers in each vertical domain are oriented at a certain canting angle φ^l with respect to the external field. Note that in the absence of the external magnetic field, the magnetization vectors in the alternating Fe layers of the multilayer will be aligned symmetrically with respect to the easy axis (Figs. 3a and b). The presence of an external in-plane magnetic field modifies this configuration (Fig. 3c). Due to the reduced symmetry, the top and bottom Fe layers experience only half of the antiferromagnetic exchange interlayer coupling energy. Therefore, the gain in Zeeman energy causes a maximal twist

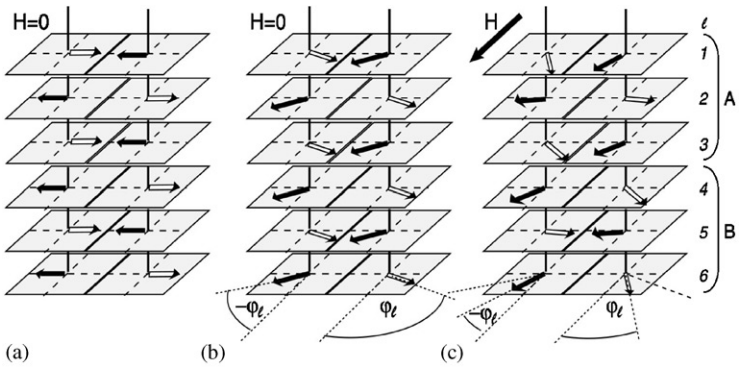

Fig. 3. Examples of magnetization configurations in a finite multilayer composed of an even number of ferromagnetic (FM) layers l antiferromagnetically coupled across non-magnetic spacers (only FM layers are shown); three possible types of domains are depicted: (a) interlayer coupling is antiferromagnetic, external magnetic field $H = 0$; (b) non-collinear configuration, canting angles $\varphi^l = -\varphi^l$, $H = 0$; c) twisted non-collinear configuration in an external magnetic field applied along the in-plane easy axis, $\varphi^l = -\varphi^l$ and $\varphi^l > -\varphi^{l-1}$. Brackets A and B indicate the two transverse anti-phase parts of one lateral domain.

in the end layers, which steadily relaxes from both sides towards the middle of the film. For an even number of magnetic layers, the magnetization vectors in the first and the last Fe layers are in anti-phase which creates a splitting in the middle of the multilayer stack. So the structure is vertically split into two parts, A and B, as shown in Fig. 3c. This leads to an unavoidable stacking fault of the parallel to the field components of magnetization vectors $\mathbf{M}^l$ in the sequence of Fe layers, which causes the appearance of the double-maximum at the $\frac{1}{2}$- and $\frac{3}{2}$-order Bragg peak positions in Fig. 2a. In contrast, a strong off-specular scattering sheet located exactly in the position of the $\frac{1}{2}$-order Bragg peak proves that there is no stacking fault in the distribution of the perpendicular to the field components of magnetization vectors $\mathbf{M}^l$ across the multilayer in each vertical domain.

Note that only two types of domains are possible once a saturation field was applied to the sample with the four-fold anisotropy. One type of domains has in the top part the structure A and in the bottom part the structure B, and the other type of domains has mirrored configuration with respect to the external field direction (see Fig. 3c). In this case it is energetically favorable that the domains have a lamellar or striped shape [18].

The quantitative analysis of both, polarized neutron specular reflection and off-specular scattering collected over a broad range of incident and scattering angles, was performed using a formalism based on the distorted wave Born approximation (DWBA) and developed in our earlier publications [15,19–21]. Within this approach we have to find first exact wave functions for the neutron interacting with a mean film potential being averaged over the lateral coordinate. Then one performs a perturbation calculation using these wave functions and the perturbation potential. In fact, this problem is just reduced to the calculation of the reflectance, which may be found via the supermatrix routine [20]. Due to a very strong surface anisotropy, the layer magnetization vectors $\mathbf{M}^l$ are aligned in planes with canting angles φ^l with respect to the direction of the external field $\mathbf{H}$. Within each layer $\varphi^l_A = -\varphi^l_B$, where indexes A and B correspond to the top and bottom parts of the multilayer stack. In this case, the mean field potential depends only on the coordinate z, perpendicular to the surface with the magnetic part being determined by the component $M^l_{II} = M^l \cos\varphi^l$ parallel to the vector $\mathbf{H}$. The perturbation potential is given by the lateral fluctuations of the magnetic moment. The components $M^l_{\text{perp}} = M^l \sin\varphi$ perpendicular to the vector $\mathbf{H}$ alternate in the neighboring domains within each layer (so that $M^l_{\text{A perp}} = M^l_{\text{B perp}}$) and also change sign from layer to layer in each domain. The magnetic scattering operator is determined by the domain form factor [20].

The result of the fit to the data based on the above-described model is shown in Fig. 2b. A remarkable agreement between theory and experiment allowed describing all details of the off-specular scattering and through this the detailed composition of the layer magnetization in the multilayers system. Parameters of the fit were the canting angle φ^l and the average domain size. The result of the fit (see Fig. 4 open circles) shows the variation of the canting angle φ^l across the 12 Fe layers of sample 1. The two outermost layers have the maximum twist (which corresponds to a smaller canting angle) towards the direction of the external field ($\varphi^1 = -\varphi^{12} = 30^\circ$). The layers next to the outermost layers have a maximum canting angle ($\varphi^2 = -\varphi^{11} = -70^\circ$) due to the strong exchange coupling interaction. The next two "couples" towards the center of the multilayer have canted angles of ($\varphi^3 = -\varphi^{10} = 35^\circ$) and ($\varphi^4 = -\varphi^9 = -65^\circ$), respectively. And, finally ($\varphi^5 = -\varphi^8 = 55^\circ$) and ($\varphi^6 = -\varphi^7 = -60^\circ$). Thus the magnetic configuration is antisymmetric with respect to the middle of the multilayer. It has maximum twist at the end layers, which is

relaxed towards the center of the film, but involves the entire sample. The average domain size obtained from the fit to the data was 2800 Å.

The distribution of the canting angles is shown in Fig. 4 (black dots) for the same sample but in the external magnetic field of 200 G [22].

The above-described sample has rather thick Fe layers of 67 Å, which assures the behavior of a "soft" ferromagnet. The second sample has 26 Å thick Fe layers. Fig. 5 shows the scattered intensity from this sample in the external magnetic field of 300 G. The 2D map contains features similar to the ones observed for sample 1. These are the doubling of the $\frac{1}{2}$-order Bragg peak with a minimum at $(p_i + p_f) = 0.078\,\text{Å}^{-1}$ and a strong off-specular Bragg sheet crossing the specular line at exactly the position of the minimum of the split Bragg reflection.

Thus our findings prove that non-uniform canted states are a general feature for exchange coupled multilayers exposed to an in-plane external magnetic fields.

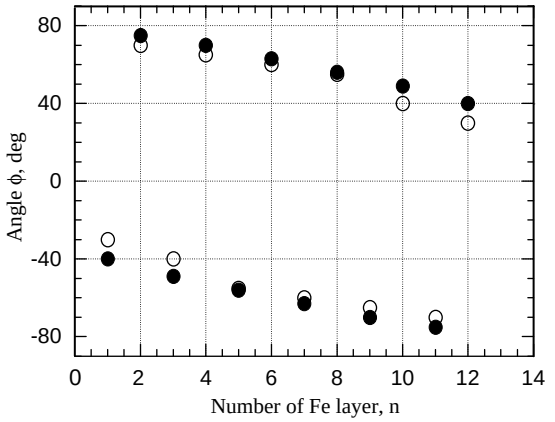

Fig. 4. Twisted canting angle φ^l as a function of Fe layer l for sample 1 in the external magnetic field H of 200 G (black dots) and 400 G (open circles).

4. Conclusions

In conclusion, the experimental evidence of the non-uniform twisted canting state in Fe/Cr superlattices in the spin-flop phase has been obtained. It is shown that the canting angles are maximal in the end layers and progressively relax towards the middle of the multilayer from both sides. The magnetic moments in the two end layers are tilted in anti-phase. This creates an unavoidable stacking fault in the middle of a multilayer stack with an even number of magnetic layers. The multilayer is decomposed into two types of vertical domains with the mirrored configuration of magnetic moments.

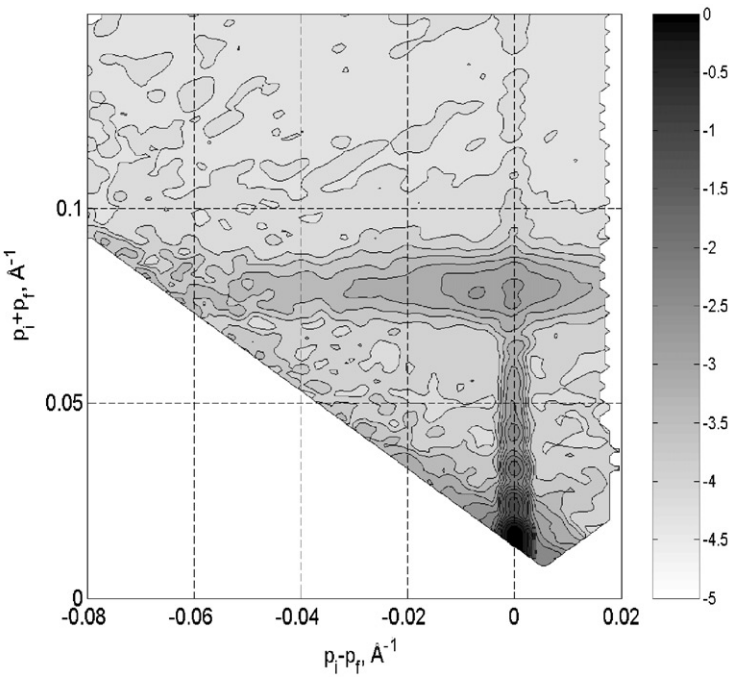

Fig. 5. Experimental 2D scattered intensity map from sample 2 in the in-plane external magnetic field of 300 G as a function of $(p_i + p_f)$ and $(p_i - p_f)$, with p_i and p_f the perpendiculars to the surface projections of incoming and scattered neutron wave-vectors, respectively. The logarithmic intensity gray-color scale is shown on the side. The incoming neutrons are in the "-" state.

Acknowledgements

The authors thank V. Leiner for assistance during the experiment and the BMBF (Grant No. 03DUOTU1/4), NATO (Grant No. PST.CLG.976169), RFBR (Grant No. 01-02-17119) and in part MST of RF for the financial support.

References

[1] M.N. Baibich, J.M. Broto, A. Fert, F. Nguyen Van Dau, F. Petroff, P. Etienne, G. Creuzet, A. Friederich, J. Chazelas, Phys. Rev. Lett. 61 (1988) 2472.
[2] G. Binasch, P. Grünberg, F. Saurenbach, W. Zinn, Phys. Rev. B 39 (1989) 4828.
[3] B. Heinrich, J.A.C. Bland (Eds.), Ultrathin Magnetic Structures II, Springer, Berlin, 1994, p. 45 (Chapter 2).
[4] Y. Yafet, in: L.H. Bennet, R.E. Watson (Eds.), Magnetic Multilayers, World Scientific, Singapore, 1994, p. 9.
[5] A. Fert, P. Grünberg, A. Barthelemy, F. Petroff, W. Zinn, J. Magn. Magn. Mater. 140-144 (1995) 1.
[6] M.D. Stiles, J. Magn. Magn. Mater. 200 (1999) 322.
[7] R.W. Wang, D.L. Mills, Phys. Rev. B 50 (1994) 3931.
[8] F.C. Nörtermann, R.L. Stamps, A.S. Carrico, R.E. Campley, Phys. Rev. B 46 (1992) 10847.
[9] R.W. Wang, D.L. Mills, E.E. Fullerton, J.E. Mattson, S.D. Bader, Phys. Rev. Lett 72 (1994) 920.
[10] A.B. Chizhik, K. Fronc, S.L. Gnatchenko, D.N. Merenkov, R. Zuberek, J. Magn. Magn. Mater. 213 (2000) 19.
[11] J.F. Ankner, G.P. Felcher, J. Magn. Magn. Mater. 200 (1999) 741.
[12] V. Lauter-Pasyuk, H.J. Lauter, B. Toperverg, O. Nikonov, E. Kravtsov, M. Milyaev, L. Romashev, V. Ustinov, Physica B 283 (2000) 194.
[13] J.A. Borchers, J.A. Dura, C.F. Majkrzak, S.Y. Hsu, R. Lolee, W.P. Parrat, J. Bass, Physica B 283 (2000) 162.
[14] V. Lauter-Pasyuk, H.J. Lauter, B. Toperverg, O. Nikonov, E. Kravtsov, L. Romashev, V. Ustinov, J. Magn. Magn. Mater. 226–230 (2001) 1694.
[15] H.J. Lauter, V. Lauter-Pasyuk, B.P. Toperverg, L. Romashev, V. Ustinov, E. Kravtsov, A. Vorobiev, O. Nikonov, J. Major, Appl. Phys. A. Mater. Sci. (2001), to be published.
[16] V.V. Ustinov, M.A. Milyaev, L.N. Romashev, T.P. Krinitsina, E.A. Kravtsov, J. Magn. Magn. Matter. 226–230 (2001) 1811.
[17] http://www.ill.fr.
[18] H.J. Lauter, V. Lauter-Pasyuk, B.P. Toperverg, L. Romashev, M. Milyaev, V. Ustinov, in preparation.
[19] B. Toperverg, Physica B 297 (2001) 160.
[20] B. Toperverg, O. Nikonov, V. Lauter-Pasyuk, H.J. Lauter, Physica B 297 (2001) 169.
[21] B.P. Toperverg, A. Rühm, W. Donner, H. Dosch, Physica B 267–268 (1999) 198.
[22] V. Lauter-Pasyuk, H.J. Lauter, B.P. Toperverg, L. Romashev, V. Ustinov, Phys. Rev. Lett. 89 (2002) 167–203.